2014 IEEE 11th International Conference on Mobile Ad Hoc and Sensor Systems

Grace: Recognition of Proximity-Based Intentional **G**roups using Coll**a**borative Mobile Devi**ce**s

Na Yu and Qi Han
Department of Electrical Engineering and Computer Science
Colorado School of Mines, Golden, CO 80401
{nyu, qhan}@mines.edu

***Abstract*—People in social environments often appear in groups to have face-to-face interactions, automatically recognizing these groups will facilitate many applications while being unobtrusive. In this work, we focus on recognizing multiple concurrent intentional groups of people in proximity using a real-time distributed approach running on commodity mobile devices. Specifically, we study Bluetooth signal strength probability distribution for proximity estimation and model the group probability distribution under Bluetooth signal strength. Further, we develop a real-time distributed group determination algorithm. We implement a prototype system on iOS platforms which includes both the group recognition service and a mobile social application using the service. Both our simulation and prototype results show that the proposed approach can recognize proximity-based intentional groups with high accuracy.**

I. Introduction

People often appear in groups in various scenarios, such as a group lunch around a table, a group conversation during a coffee break or reception at a conference, a brainstorm session in a meeting room. One common characteristic of these scenarios is that people are physically close to each other, facing each other or a common object for face-to-face interactions. In addition, there may be multiple concurrent groups at the same location. For instance, people voluntarily form many small groups at a poster session at a conference; a workshop organizer may divide researchers into several different groups depending on their research interests and ask each group to stay in one corner of a room to brainstorm on a designated topic. Unobtrusively recognizing these proximity-based intentional groups can benefit a variety of applications for group members. For instance, contact information can be automatically shared among group members for future correspondence, a common available time slot can be automatically identified for a future gathering, an article highly relevant to the conversation can be automatically sent to each group member, a notification of a future event related to this group's interest will be disseminated within the group.

With the increasing popularity of sensor-equipped mobile devices, automatic recognition of proximity-based intentional groups now becomes possible. Proximity-based group recognition has been studied before using a centralized approach [1] [2] or a peer-to-peer approach [3]. Nevertheless, the existing approaches need to trace all the users' movement for a certain time period in order to group co-moving users. *What distinguishes our work from existing work is that we aim to group co-located users regardless of their mobility.* In outdoor environments, GPS coordinates can be used to detect co-located users, but it is hard to separate co-located groups due to the resolution of GPS (even high-quality GPS SPS receivers can only provide a horizontal accuracy of 3 meters [4]). In indoor environments, WiFi fingerprints can be used to detect co-located users using indoor localization techniques such as [5]; however, this requires infrastructure support and hence is not applicable in many outdoor environments. In contrast, we would like our approach to separate co-located groups in an infrastructure-free environment for both indoor and outdoor environments by purely relying on sensors built in commodity mobile devices.

We are faced with several interesting challenges. First, how to accurately infer proximity among co-located users. Existing work has used acoustic signals to measure distances between mobile devices [6] [7]. However, a central server or a master node is usually required to schedule the emission of acoustic signals on all devices. This is impractical in an infrastructure-free or a multi-group environment, since users may form arbitrary groups anytime and anywhere. We choose to use Bluetooth Received Signal Strength Indication (RSSI) to estimate the relative distance between mobile device users and use Bluetooth peer-to-peer communication to collaboratively form groups. However, Bluetooth is not accurate when used to measure distances. Second, how to distinguish multiple concurrent proximity-based intentional groups. When people in different co-located groups are in proximity, it is hard to separate them using the Bluetooth RSSI between their mobile devices. Third, groups need to be recognized in real-time. Consider the above conference scenario, for people who happen to meet each other and want to exchange their contact information, the grouping process should be done in seconds by extracting instant sensor data or pattern from the mobile devices. Therefore, proximity-based intentional groups should be recognized in real-time and in a distributed manner for mobile applications.

Problem Definition: A proximity-based intentional group is a set of people who are close to each other (i.e., within Bluetooth communication range) with the intention of having face-to-face interactions. We aim to identify multiple concurrent proximity-based intentional groups in real-time using Bluetooth RSSI in an infrastructure-free environment irrespective of whether the groups are stationary or mobile.

978-1-4799-6036-1/14 $31.00 © 2014 IEEE
DOI 10.1109/MASS.2014.11

In this work, we first study proximity estimation based on Bluetooth RSSI probability distribution under different communication scenarios. We then model the group probability distribution under Bluetooth RSSI. Using the group probability distribution model, we propose a real-time distributed group determination algorithm. We also present a prototype system called Grace, which implements the proposed approach on iOS 7.0 devices and also includes a contact information exchange application using the group identification service. Our evaluation is conducted via both simulations and the Grace prototype system. The simulation results show that our approach works desirably for a variety of group scenarios in terms of density and closeness of groups and is scalable when the number of groups increases. The actual deployment results show that the system achieves high accuracy when there is a significant difference of proximity or blocking obstacle effect between intra-group and inter-group.

II. An Exploratory Study of Bluetooth Signal Characteristics

Bluetooth signal propagation has been studied in terms of path loss effect and multipath effect. Different models have been developed for the impact of path loss and multipath separately.

A. Path Loss Effects on Bluetooth Signals

A widely adopted Bluetooth radio propagation model [8] is shown in Formula 1.

$$P_{RX} = P_{TX} + G_{TX} + G_{RX} + 20log(\frac{c}{4\pi f}) - 10nlog(d), \quad (1)$$

where P_{RX} is the received power level, P_{TX} is the transmitted power, G_{RX} and G_{TX} are the antenna gains, c is the speed of light ($3.0 \times 10^8 m/s$), f is the central frequency (2.44 GHz), n is the attenuation factor (e.g., 2 in free space), and d is the distance (in meter) between the transmitter and the receiver. However, this model is only a theoretical reference and it does not take into consideration impact of obstacles. We next study how obstacles affect Bluetooth signal propagation. All the experiments used iPhones and iPads with Bluetooth 4.0 and iOS 7.0.

The obstacle we study is specific to human body blocking effect as mobile devices are carried by people. Existing work [9]–[12] has observed that human body has a significant impact on WiFi signals (in both 2.4 GHz and 5 GHz frequencies). Since Bluetooth also uses 2.4 GHz frequency, we infer that similar obstacle effect of human body on WiFi signals is also applicable to Bluetooth signals. To verify our hypothesis, we conduct the following experiments using the two scenarios both indoors and outdoors: Fig. 1 (a) shows the scenario with Line-of-Sight (LOS) signal propagation between the devices of Alice and Bob, and Fig. 1 (b) shows the scenario with possible blocking by Bob.

Signal attenuation when changing device orientation. In this set of experiments, we compare the RSSI patterns of the two scenarios above, where the distance between Alice's and Bob's devices is 1 meter. (1) For the LOS scenario in Fig. 1 (a), Alice holds her mobile device right in front of her, and Bob starts holding his mobile device directly facing Alice's mobile device (i.e., at the angle of 0 degree). At each step, Bob rotates his mobile device by 15 degrees clockwise. We observe that the Bluetooth RSSI patterns on both Alice's and Bob's mobile devices are the same and the RSSI is almost constant even when the angle between the two devices varies (Fig. 2 w/o human shield). (2) For the obstacle scenario in Fig. 1 (b), Alice holds her mobile device right in front of her, and Bob also holds his mobile device right in front of him at each step. But instead of rotating the mobile device, Bob himself turns by 15 degrees clockwise at each step and he also adjusts his position in order to keep the 1 meter distance between Alice. We observe that the RSSI patterns on both mobile devices are still the same: the Bluetooth signal is significantly blocked by the human body within about 90 degrees, i.e., between the angle of 135 degree and the angle of 225 degree (Fig. 2 w/ human shield). This is similar to the 90 degrees blocking sector model of human body for WiFi signals [9]. We also observe that the RSSI values on Alice's mobile device are slightly lower (about 2 dBm less) than those on Bob's. This is because the blocking effect is more significant when the obstacle is closer to the transmitter. Since the distance between two devices is short, the position of the human shield (whether it is closer to the transmitter or receiver) does not affect signal attenuation much (typically 2 dBm less), this impact can be ignored. In addition, our experiments also show that there is almost no difference if the signal crosses multiple persons or just one single person, the same findings as in [9]. Finally, we observe similar trends for both indoor and outdoor environments, so we only show the results for indoor environment here. In summary, all these empirical results validate our hypothesis that there exists obstacle effect of human body on Bluetooth RSSI.

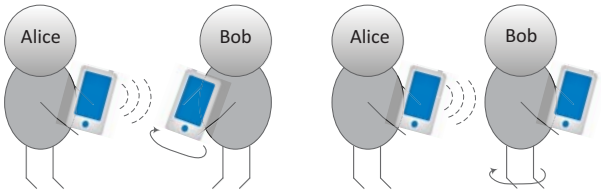

(a) w/o human shield (i.e., LoS) (b) w/ human shield (i.e., obstacle effect)

Fig. 1. Scenarios used for exploratory study of Bluetooth signal propagation

Signal attenuation over distance. In this set of experiments, we study how obstacle affects Bluetooth signal propagation at different distances. We also compare the RSSI patterns of the two scenarios in Fig. 1. Instead of rotation, we only use the position at the angle of 0 degree in Fig. 1 (a) while use the position at the angle of 180 degree in Fig. 1 (b). These fixed relative positions result in regularized signal attenuation patterns due to path loss over distances. These regularized patterns will be further utilized in the RSSI probability distribution model in the next section. For both scenarios, we measure the average RSSI values for each

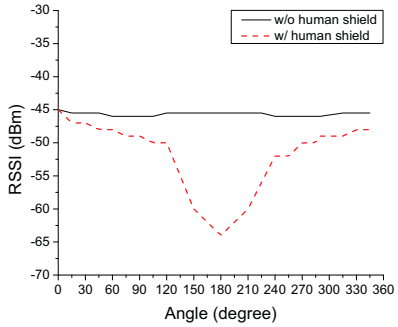

Fig. 2. Impact of angle between two devices on Bluetooth RSSI (indoor)

distance using thousands of samples obtained at different times. Fig. 3 shows the RSSI patterns for indoor environments (the results for outdoor environment are not shown here due to the similar trend), where each vertical line represents the standard deviation of the samples at each distance. We observe that the RSSI values with human shield are much lower than those without human shield, especially for smaller distances. Again, this verifies the existence of the human shield effect on Bluetooth RSSI over distances.

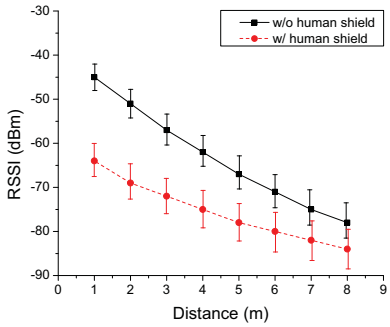

Fig. 3. Impact of distance between devices on Bluetooth RSSI (indoor)

B. Multipath Effect on Bluetooth Signals

According to existing work [13], Bluetooth RSSI probability distribution at a single reference point follows Weibull distribution [14]. Using the probability density function of the Weibull distribution, we can calculate the probability of an RSSI range $[\theta_l, \theta_h)$ as shown in Formula 2:

$$P(\theta_l \leq rssi < \theta_h) = e^{-(\frac{\theta-\theta_h}{\lambda})^k} - e^{-(\frac{\theta-\theta_l}{\lambda})^k}, \qquad (2)$$

where parameters k, λ, and θ can be calculated using the mean and standard deviation of the RSSI samples [13] [15]. However, this probability function is only for a single reference point without considering path loss effect.

To the best of our knowledge, there is no existing model that combines the RSSI probability distribution (i.e., multipath model in Formula 2) with the signal attenuation patterns over distances (i.e., path loss model in Formula 1). Instead of attempting to build such an integrated model, we decide to apply both the RSSI probability distribution and the signal attenuation patterns to estimate the theoretical thresholds that can be used to separate different groups.

We realize that the results shown in Fig. 2 and Fig. 3 only capture the signal properties in the specific environment of our experiments. When the environment changes, the RSSI values will change but still have the same trend. Our focus of this work is not building a general Bluetooth signal propagation model to fit a variety of environments. However, this issue can be solved by performing calibration on the scene, i.e., use the newly obtained RSSI values to reset the key parameters in our approach. We will consider the approach for calibration in our future work.

III. Group Identification using Bluetooth Signal Information

According to our notion of proximity-based intentional groups, for people in the same group, their mobile devices satisfy LOS communication. However, if two users belong to two different groups, their distance can be larger while their mobile devices may suffer from human shield.

A. Basic Ideas

We next explain how the empirical findings of human shield effect can be used in combination with the multipath effect model (Formula 2) to derive a group model. Although Formula 2 is for a single reference point, we observe that a single set of parameters k, λ, and θ is applicable to all reference points at a given distance when the LOS or human shield condition is given. Therefore, we can use the mean and standard deviation of the RSSI samples at each distance as shown in the signal attenuation patterns in Fig. 3 to calculate the RSSI probability distribution for each distance, with or without human shield, respectively. The values as shown in the figure can be calibrated in different environments.

We can set a distance threshold for users inside a group, e.g., the 2 meters social distance [16]. Then, the probability distribution of the RSSI value for group members is the RSSI probability distribution inside an area within the distance threshold. Since there is no existing RSSI probability distribution model over distances, we estimate the probability distribution inside an area using a discrete method. For a distance range $(d_l, d_h]$, we can divide it into smaller ranges, i.e., increase Δd at each step. For a given RSSI range, its probability p_n at the nth distance step $d_l + n \times \Delta d$ can be calculated using Formula 2. The corresponding probability p across the distance range $(d_l, d_h]$ can be estimated using Formula 3, where $\frac{(2n-1)(\Delta d)^2}{(d_h)^2-(d_l)^2}$ is the probability of the nth distance step inside the distance range $(d_l, d_h]$.

$$p = \sum_{n=1}^{\frac{d_h-d_l}{\Delta d}} \frac{p_n(n^2-(n-1)^2)(\Delta d)^2}{(d_h)^2-(d_l)^2} = \sum_{n=1}^{\frac{d_h-d_l}{\Delta d}} \frac{p_n(2n-1)(\Delta d)^2}{(d_h)^2-(d_l)^2} \qquad (3)$$

Based on the estimated RSSI probability distribution across a distance range, we can further estimate the RSSI probability distribution within a distance threshold as the intra-group RSSI probability distribution and the RSSI probability distribution

outside the distance threshold (i.e., from the distance threshold to Bluetooth transmission range) as the inter-group RSSI probability distribution. Further, we include the possibility of human shield in the estimation of inter-group RSSI probability distribution. These estimations will then be used to build the probability-based group model.

B. Group Probability Distribution under Bluetooth RSSI

Let $R_{i,j}$ be the variable representing Bluetooth RSSI received at user j from user i, $d_{i,j}$ be the actual distance between the two users, $s_{i,j}$ is a Boolean variable to indicate whether there is human shield between their Bluetooth communication (0 represents no, 1 represents yes), and $G_{i,j}$ is a Boolean variable to indicate whether they are in the same group (0 represents no, 1 represents yes).

Assume that the maximum intra-group distance (i.e., minimum inter-group distance) is D_{max}, then we have a set of conditional probabilities given that the group relationship is known as shown in Formula 4,

$$\begin{cases} P(d_{i,j} \leq D_{max}, s_{i,j} = 0 | G_{i,j} = 1) = 1 \\ P(d_{i,j} > D_{max}, s_{i,j} = 1 | G_{i,j} = 0) = x \\ P(d_{i,j} > D_{max}, s_{i,j} = 0 | G_{i,j} = 0) = 1 - x \end{cases} \tag{4}$$

where x is the probability that the Bluetooth communication between users i and j suffer from human shield.

As discussed in Section II, both existing work and our preliminary experiments show that the angle of human shield is about 90 degrees. Therefore, the probability of a user who is human shield for the communication of his own mobile device is 1/4, then the probability that the communication between two users suffers from human shield is $1-3/4\times3/4 = 7/16$. Although the wireless signal attenuation closer to the signal transceiver is theoretically larger than being further away from the signal source, we observe that the difference is not significant over the short Bluetooth range. Further, we also observe that the difference is not significant if the signal crosses through multiple persons. Therefore, the human shield probability here only takes equal consideration of the shield on the transceiver side and the receiver side, that is $x = 7/16$.

Next, we look at the conditional probability distribution of RSSI given that the group relationship is known. Based on Formula 4, we can derive Formulas 5 and 6.

$$P(R_{i,j} = r | G_{i,j} = 1) = P(R_{i,j} = r | d_{i,j} \leq D_{max}, s_{i,j} = 0) \tag{5}$$

$$\begin{aligned} &P(R_{i,j} = r | G_{i,j} = 0) \\ &= (1-x) \times P(R_{i,j} = r | d_{i,j} > D_{max}, s_{i,j} = 0) \\ &\quad + x \times P(R_{i,j} = r | d_{i,j} > D_{max}, s_{i,j} = 1) \end{aligned} \tag{6}$$

Further, using Bayes' theorem, we can derive Formula 7.

$$\begin{aligned} &P(G_{i,j} = y | R_{i,j} = r) \\ &= \frac{P(R_{i,j} = r | G_{i,j} = y) \times P(G_{i,j} = y)}{\sum_{y=0}^{1} P(R_{i,j} = r | G_{i,j} = y) \times P(G_{i,j} = y)} \end{aligned} \tag{7}$$

Without prior knowledge of the group relationship, we can assume that whether two users belong to the same group or not has equal probability, i.e., $P(G_{i,j} = 0) = P(G_{i,j} = 1) = 0.5$. Therefore, Formula 7 becomes Formula 8.

$$\begin{aligned} &P(G_{i,j} = 1 | R_{i,j} = r) \\ &= \frac{P(R_{i,j} = r | G_{i,j} = 1)}{P(R_{i,j} = r | G_{i,j} = 1) + P(R_{i,j} = r | G_{i,j} = 0)} \end{aligned} \tag{8}$$

By varying D_{max} from 1 meter to m meters within Bluetooth transmission range, we can derive these three conditional probabilities in the same way: $P(R_{i,j} = r | d_{i,j} \leq D_{max}, s_{i,j} = 0)$, $P(R_{i,j} = r | d_{i,j} > D_{max}, s_{i,j} = 0)$, and $P(R_{i,j} = r | d_{i,j} > D_{max}, s_{i,j} = 1)$.

$P(R_{i,j} = r | d_{i,j} \leq D_{max}, s_{i,j} = 0) =$

$$\begin{cases} Pa_1, & \text{if } r \geq TH_1 \\ Pa_2, & \text{if } TH_2 \leq r < TH_1 \\ ... & \\ Pa_{m-1}, & \text{if } TH_m \leq r < TH_{m-1} \\ 1 - \sum_{k=1}^{m-1} Pa_k, & \text{if } r < TH_m \end{cases} \tag{9}$$

$P(R_{i,j} = r | d_{i,j} > D_{max}, s_{i,j} = 0)$ and $P(R_{i,j} = r | d_{i,j} > D_{max}, s_{i,j} = 1)$ are similar to Formula 9 except that Pa_k is replaced with Pb_k and Pc_k, respectively. Each of these values are calculated using Formula 3. The RSSI range thresholds TH_1, TH_2, ..., TH_m are the mean RSSI values over LOS 1 meter, 2 meters, ..., and m meters, respectively (as shown in Fig. 3). In addition to these range thresholds, there is also a boundary threshold TH_w for getting rid of weak signals (i.e., $R_{i,j} < TH_w$) relative to D_{max}. The value of TH_w is determined by $P(R_{i,j} \geq TH_w) = 1 - e^{-(\frac{\theta - TH_w}{\lambda})^k} \geq 0.99$, using Formula 2 based on the Weibull distribution over LOS D_{max}.

Finally, we can derive $P(G_{i,j} = 1 | R_{i,j} = r)$ and it is in the same form as Formula 9 except that Pa_k should be replaced with P_k. According to Formula 8, $P_k = \frac{Pa_k}{Pa_k + (1-x) \times Pb_k + x \times Pc_k}$.

C. Probability-Based Group Determination

We consider that two users are in the same group if and only if both of them determine each other as a group member, so we calculate the probability that two users are in the same group based on bi-directional RSSI values between them. Therefore, given RSSI values $R_{i,j}$ and $R_{j,i}$, the two users i and j can determine their group probability as using Formula 10. When a user has multiple possible groups, then the group in which the user has the highest probability is selected.

$$P(G_{i,j} = 1) = P(G_{i,j} = 1 | R_{i,j}) \times P(G_{i,j} = 1 | R_{j,i}) \tag{10}$$

The probability that user i is in group I is as shown in Formula 11, where N_i is the set consisting of user i's neighbors. This means that the group probability between a user and all neighbors are considered when determining the

probability that the user belongs to a group.

$$P(U_i \in G_I) = \prod_{\forall U_j \in G_I, j \neq i} P(G_{i,j} = 1) \prod_{\forall U_j \in N_i, U_j \notin G_I} P(G_{i,j} = 0) \tag{11}$$

Consider the scenario depicted in Fig. 4 where user 3 has three possible groups, i.e., $G_I = \{U_1, U_2, U_3\}$, $G_{II} = \{U_2, U_3, U_4\}$, and $G_{III} = \{U_3, U_{10}\}$.

$$P(U_3 \in G_I) = P(G_{1,3} = 1) \times P(G_{2,3} = 1) \times P(G_{3,4} = 0) \times P(G_{3,10} = 0)$$

$$P(U_3 \in G_{II}) = P(G_{1,3} = 0) \times P(G_{2,3} = 1) \times P(G_{3,4} = 1) \times P(G_{3,10} = 0)$$

$$P(U_3 \in G_{III}) = P(G_{1,3} = 0) \times P(G_{2,3} = 0) \times P(G_{3,4} = 0) \times P(G_{3,10} = 1)$$

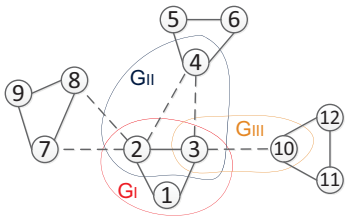

Fig. 4. An example scenario that a user belongs to multiple possible groups

Our group determination algorithm as shown in Algorithm 1 uses the group probability (e.g., $P(U_i \in G_I)$) as a metric for group selection. The algorithm runs on each user's mobile device, and it requires the 2-hop neighborhood information of the user. The 2-hop neighborhood information collection can be done by first collecting 1-hop neighbors and then sending the 1-hop neighborhood to all neighbors via Bluetooth peer-to-peer communication before running the algorithm. The detailed process will be discussed in Section V. The reason of collecting 2-hop neighborhood information is that it is practical to provide enough information in a peer-to-peer system. The number of hops is actually a tradeoff between accuracy and efficiency, i.e., the more hops of neighborhood information we have, the more accurate the results can be but at higher overhead.

Node exclusion in the algorithm (step 11) makes sure that each user only joins one group at a time. When a user has a high probability of belonging to multiple groups, we do not merge the groups. Instead, we choose the group with the highest probability (maybe part of an existing group) for the user, allowing false-negative (i.e., users being falsely identified as not belonging to a certain group) rather than false-positive (i.e., users being falsely identified as belonging to a certain group) to be on the safe side. In most cases, this step can lead all users to make consistent group decisions since users which may choose different groups are excluded. However, inconsistency still exists when a user which should be excluded is not excluded due to missing links caused by connectivity issues or incomplete information to compute cliques in the 2-hop neighborhood. To achieve consistent groups for all users, we add one more step to send the group which has been determined locally to all other group members. Upon receiving the groups from other members in the locally determined group (ignore the groups from non-members), the user compares all the groups with the locally determined group. The locally determined group is finally identified as a consistent group for all its members if and only if all its members have exactly the same locally determined group. Again, this is to make sure that groups are identified on the safe side. The worst case time complexity of the Bron Kerbosch algorithm is $O(3^{n/3})$ with n being the number of nodes in the local graph, the algorithm may be replaced with a more efficient one.

Algorithm 1 : Probability-Based Group Determination

Input: a local graph representing a user's two-hop neighborhood
Output: maximum complete subgraph in which the user has highest group probability

1: Start from the node representing the current user in the local graph, find all maximum complete subgraphs containing this node using the Bron Kerbosch algorithm [17].
2: **if** more than 1 maximum complete subgraphs **then**
3: **for** all maximum complete subgraphs **do**
4: Calculate the probability that the user is in the group of this subgraph;
5: **end for**
6: Select the maximum complete subgraph with the largest probability as the group for the user;
7: **end if**

8: **for** all other nodes in this maximum complete subgraph **do**
9: Find all other maximum complete subgraphs containing it;
10: **if** the node has a maximum complete subgraph with higher probability than the current one **then**
11: Exclude this node from the group of the original maximum complete subgraph;
12: **end if**
13: **end for**
14: Include the remaining nodes in the group of the user;

Using the example in Fig. 4, the input on user 3's mobile device is the local graph containing his 2-hop neighborhood, i.e., include all users except user 9. Assume that in Fig. 4, the shorter the edge between two nodes, the higher the group probability between the two users. Then, user 3 selects group G_I among those three possible groups. Since user 2 has the highest group probability in group G_I among its three possible groups, it remains in user 3's group. Therefore, the output of user 3's group contains three users as shown in group G_I. In the meantime, each other user runs the same algorithm and determines the group separately. Finally, all the users can exchange their groups to reach a consensus.

IV. Performance Evaluation via Simulations

To evaluate our approach, we first use simulations to validate the proposed probability-based group model and group determination algorithm in various settings including scalability testing. In the next section, we will present how we implement the Grace system and how it works in actual settings. As discussed in Section VI, existing work recognizes groups based on various behaviors such as social interactions, activity similarity, or proximity. The existing work of proximity groups [1] is the most relevant to our work, but it is not focused on intentional groups in which people are intended to have

face-to-face interactions. To the best of our knowledge, there is no existing work that identifies proximity-based intentional groups. Therefore, we cannot compare our approach with any of the existing approaches.

A. Simulation Setup

We implement a C++-based simulator which includes a topology generator, a Bluetooth RSSI generator based on the RSSI probability distributions, the group probability model, and the group determination algorithm. For the group determination algorithm, we implement the probability-based group determination algorithm and also a value-based group determination algorithm for comparison. In the value-based group determination algorithm, we replace the group probability metric in Algorithm 1 with a metric representing the average RSSI value with other group members in a candidate group. The specific modifications of Algorithm 1 are: 1) in line 4, calculate the the average RSSI with other users in the group of the subgraph; 2) in line 6, select the maximum complete subgraph in which the user has the largest average RSSI with other users as the group for the user; 3) in line 10, change the probability in the condition to average RSSI.

In each simulation, the simulator first generates random groups based on the inputs of the number of groups and the maximum intra-group distance. The position of each user is also randomly generated in each group based on the maximum intra-group distance and a random number of group members (i.e., 2 - 10). Then, the Bluetooth RSSI values are generated using the corresponding probability function based on the distance and existence of human shield.

We vary the intra-group distance threshold (i.e., the maximum intra-group distance, which is also the minimum inter-group distance) and the number of groups, respectively, and we aim at studying their impacts on the grouping performance. We use three performance metrics, including precision (i.e., the number of correct groups which are identified exactly the same as the actual groups over the totoal number of identified groups), recall (i.e., the number of correct groups over the total number of actual groups), and the group membership similarity (i.e., the average Jaccard similarity [18] between an identified group and the corresponding actual group). In all the results, each point is based on at least 10 simulations, and the vertical line represents the 95% confidence interval.

B. Simulation Results

We first investigate the choice of the most appropriate intra-group distance threshold indoors (Fig. 5) and outdoors. Results for outdoors are omitted due to page limitations but trends observed are similar to those indoors. As the maximum intra-group distance increases, the precision decreases, and the recall also has a decreament trend although it varies at the beginning. All these are because of the increased RSSI uncertainty over longer distances, leading to more inconsistency in the local group determination of different users. Nevertheless, both the precision and recall of the probability-based approach are higher than those of the value-based approach, showing that the probability-based approach is more effective in identifying groups over various distances. Further, the group membership similarity of the probability-based approach is also higher than that of the value-based approach. Although the group membership similarity decreases when the maximum intra-group distance decreases, the probability-based approach leads to a much smaller decrement than the value-based approach does, showing that the probability-based approach is more accurate in identifying groups over various distances. In addition, outdoor environments generally have trends similar to indoor environments, but have a larger variation in the group membership similarity over different distances. This is because the RSSI values have a larger variance (i.e., standard deviation) in outdoor environments due to different weather conditions at different times. For both indoor and outdoor environments, the maximum intra-group distances no more than 3 meters are all appropriate for the probability-based approach (i.e., with both the precision and the group membership similarity above 90%).

We then perform scalability testing by increasing the number of concurrent groups indoors (Fig. 6) and outdoors. Results for outdoors are omitted due to page limitations but trends observed are similar to those indoors.

In these tests, we have set the intra-group distance threshold to be 2 meters. As the number of concurrent groups increases, both the precision and recall of the probability-based approach are always higher than those of the value-based approach. We also observe that the impact on the group membership similarity of the probability-based approach is much less significant than on that of the value-based approach. Even when the number of groups increases to be 25, the group membership similarity of the probability-based approach still remains above 90%. Therefore, the probability-based approach is more scalable to a large number of groups.

In summary, the simulation results indicate that the probability-based approach performs much better than the value-based approach and a reasonable small intra-group distance threshold can be chosen.

V. Prototype Implementation and Evaluation

To evaluate how Grace works in realistic settings, we implement Grace on iOS platforms using objective-C. In this prototype, we would like to demonstrate that Grace can work as an unobtrusive group recognition service along with other common activities performed by a group of people to show their intent. The value of Grace in this case is to differentiate groups that perform the same activity at the same time. The software architecture of the prototype is shown in Figure 7.

The activity recognition module utilizes sensors such as accelerometer to detect user activity. In this implementation, we choose hand gestures as the activity to be recognized. More specifically, we use the uWave gesture recognition library [19] that only uses accelerometer. uWave supports eight hand gestures holding mobile devices, i.e., zigzag, square, right, left, up, down, left circle, and right circle. The group recognition

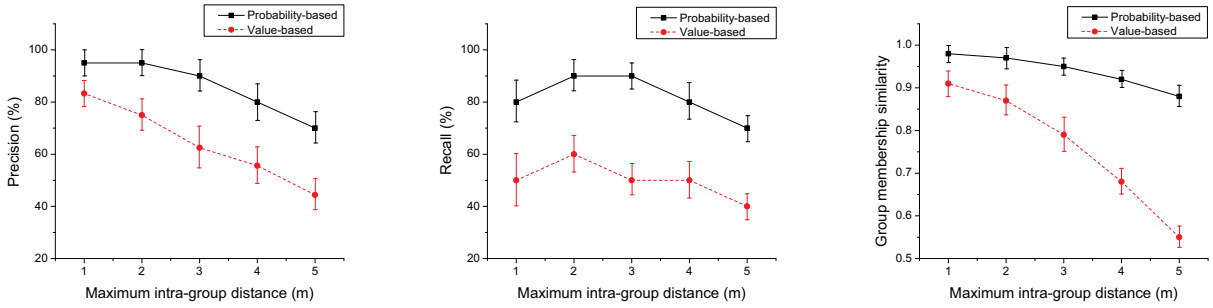

(a) (b) (c)

Fig. 5. Impact of intra-group distance threshold in indoor environments (number of groups is 10)

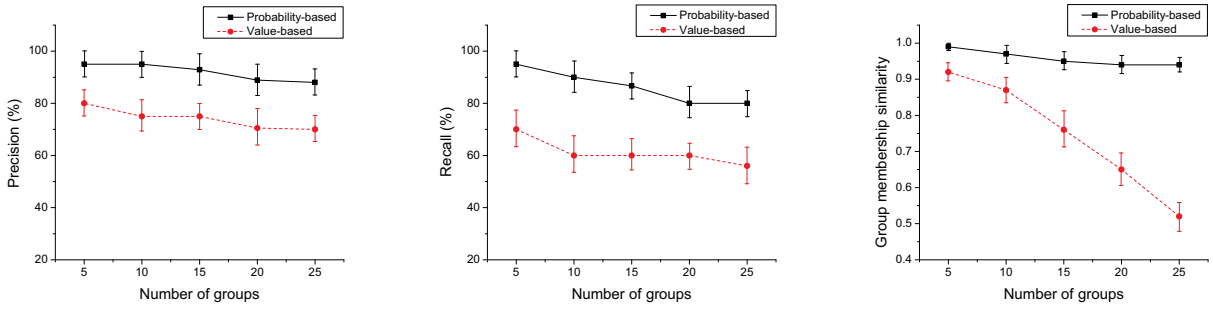

(a) (b) (c)

Fig. 6. Impact of group count in indoor environment (intra-group distance threshold is 2 meters)

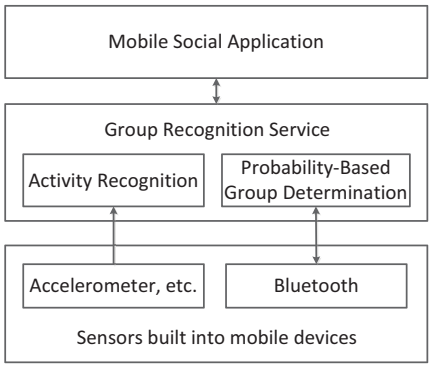

Fig. 7. Software architecture of the Grace prototype

service first discovers neighbors based on the recognized activity and then uses the probability based group determination module to determine the group members among the neighbors who have the same activity. On top of the group recognition service, we have also implemented an application that shares contact information among the identified group members who perform the same hand gesture using their mobile devices at the same time. This is a decentralized version and an extension of the Bump application [20] by allowing more people to be involved and also allowing more gestures rather than just bumping their devices.

We next analyze the latency incurred in the process. The entire process of running the contact sharing application involves: (1) recognizing and advertising the hand gesture (about $T_{gesture}$); (2) advertising neighbors with the same hand gesture (about $T_{neighbor}$); (3) further advertising neighbor information including the bi-directional RSSI values (about $T_{neighbor}$); (4) advertising the locally determined group to achieve group consistency (about T_{group}). We observe that 5 seconds are enough for each of $T_{gesture}$, $T_{neighbor}$, and T_{group}. Therefore, the entire process needs approximately $T_{gesture} + 2 \times T_{neighbor} + T_{group} = 20$ seconds. This should be faster than letting each user manually input all other users' contact information.

We have conducted experiments using six iPhone/iPad devices to test the Grace system. For both indoor and outdoor environments, we tested the scenarios shown in Fig. 8 - 9, where d_i represents the pairwise intra-group distance and d_o represents the inter-group distance in the experiments. Although we mark each intra-group link d_i and each inter-group link as d_o, it does not imply that the distance between each pair of users need to be same. Instead, it is sufficient as long as d_i for each pair is no larger than the intra-group distance threshold D_{max} and d_o for each pair is larger than D_{max}. For each different experiment, we repeat it 20 times. Then, we calculate the success ratio that all groups are identified correctly over the repeated experiments.

Test 1: multiple concurrent groups with different hand gestures. In this set of experiments, six users each holds an iPhone or iPad in front and face the devices of other users who are in the same group, and all the users start the contact sharing application at the same time but each group selects a different hand gesture. We observe that in both the two-group

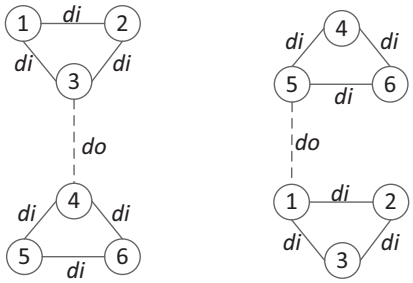

(a) w/ human shield (b) w/o human shield

Fig. 8. Testing scenario: two groups

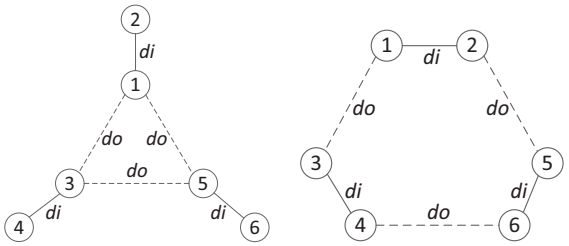

(a) w/ human shield (b) w/o human shield

Fig. 9. Testing scenario: three groups

and three-group scenarios, regardless whether it is indoor or outdoor, with or without human shield, or any intra-group distance within the Bluetooth transmission range, the groups are always correctly identified. Therefore, the system works desirably with hand gesture recognition.

Test 2: multiple concurrent groups with the same hand gestures and with human shield. In this set of experiments, we use the topologies in Fig. 8 (a) and Fig. 9 (a). We observe the same results for both topologies in both indoor and outdoor environments. When each intra-group pair distance is no larger than 1m, the group detection accuracy is 95% when inter-group pair distance is around 1.5m, but increases to be 100% when the inter-group pair distance increases to be 2m. Similarly, When each intra-group pair is no larger than 2m, the group detection accuracy is 90% when inter-group pair distance is around 2.5m, but increases to be 95% when the inter-group pair distance increases to be 3m. All these indicate that the system performs better when the intra-group distance is small comparing to the inter-group distance. Even when the intra-group and inter-group distances are not significantly different, the system still works well in the presence of human shield between groups.

Test 3: multiple concurrent groups with the same hand gestures but without human shield. In this set of experiments, we use the topologies in Fig. 8 (b) and Fig. 9 (b). Unlike in Test 2, the results are slightly different for the two topologies. (1) When each intra-group pair distance is no larger than 1m and inter-group pair distance is no smaller than 2m, in the two-group scenario, the recognition accuracy is 100% in indoor environments and is 95% in outdoor environments. This is almost the same as in Test 2 due to the significant difference between intra-group and inter-group distances. However, in the three-group scenario, the group recognition accuracy falls to 90% in both indoor and outdoor environments. This is because the distances among all pairs of users are not significantly different in this ring topology and the RSSI values are not significantly different without human shield as the blocking obstacle between groups. (2) When each intra-group pair distance is no larger than 2m and inter-group pair distance is no smaller than 3m, in the two-group scenario, the accuracy is 90% in both indoor and outdoor environments. This is also because of the insignificant distances and in absence of human shield. Then, in the three-group scenario, the accuracy further falls to 80% in both indoor and outdoor environments. The results could get even worse when we increase d_i. All these imply that d_i and d_o significantly affect the accuracy of the grouping results. This is consistent with the findings of the impact of intra-group distance threshold in the simulations.

In summary, the system can correctly identify all groups when the groups are significantly separated by distance or human shield. In other cases, some groups are not identified correctly due to a few incorrect group relationships identified between pairs of users (i.e., the existence of inconsistent group decisions presented in Section III). In general, the system leads to a high accuracy above 90%.

VI. Related Work

Group behavior recognition has been studied using mobile devices such as smartphones. In general, group behavior is recognized based on interaction [21], similarity [22], or proximity [1] [2]. However, all these approaches are centralized. They are not applicable to all scenarios. Distributed approaches such as [23] have also been developed for group recognition. Group activities are recognized using belief propagation among mobile devices [24]. It understands what the activity is and also who are involved in the activity. For each group activity, each mobile device estimates its belief given current sensor observations, and then exchanges this information with its neighbors. All devices then iteratively update and re-propagate their beliefs. Finally, the groups are distinguished by different activities. In contrast, another piece of work [3] is focused on group affiliation detection in multi-group environments, where the goal is to recognize multiple groups rather than understanding what are the group activities. Here, a peer-to-peer group affiliation method is proposed by modeling the sensor data on each mobile device as a distribution and then calculating the disparity as the Jeffrey's divergence between models from different mobile devices. Finally, the groups are distinguished based on the disparity of sensor data distributions.

In the literature, WiFi and Bluetooth are widely used for proximity estimation and indoor positioning based on mobile devices. For examples, [25] utilizes both WiFi and Bluetooth RSSI to calculate distance between two devices for relative positioning since the RSSI from a single radio has large error (e.g., 3.4 meters' average error using Bluetooth and 3.91 meters' average error using WiFi); [26] utilizes Bluetooth and combines Pedestrian Dead Reckoning (PDR) to estimate position relation between two pedestrians; [27] also

utilizes Bluetooth and PDR to provide relative positions of surrounding people in the crowd and identify groups of people who move together. However, since PDR is not applicable to identify a group of people who are not moving, and using WiFi to assist proximity estimation consumes much more energy, a better solution is to use only Bluetooth but improving its accuracy. Recently, [28] proposes a proximity estimation model which can accurately identify face-to-face proximity (i.e., 1-1.5 meters) using Bluetooth, with error rate less than 10% for all scenarios. The proposed model calculates the probability that an RSSI value indicates face-to-face proximity, but it is simply calculated based on uniform distribution. This is not accurate since the RSSI distribution is actually a much more complicated distribution which is based on the well known Rayleigh distribution. As a result, although this proximity estimation model works for face-to-face proximity, it may not be able to identify other social distances (e.g., 0.5, 2, or 3 meters).

VII. Conclusion

In this paper, we present a real-time distributed approach to distinguish multiple concurrent proximity-based intentional groups using only sensor-equipped mobile devices. We have first studied the feasibility of proximity estimation based on Bluetooth RSSI probability distribution under different communication scenarios, i.e., with/without human shield and indoor/outdoor. We have then modeled the group probability distribution under Bluetooth RSSI by applying Bayes' theorem based on the Bluetooth RSSI probability distributions. Further, we have proposed a group determination algorithm based on the group probability distribution model to collaboratively recognize the intentional groups in real-time. Finally, we have evaluated the proposed approach using both simulations and prototype implemented in iOS 7.0. The simulation results show that our approach works desirably for a variety of maximum intra-group distances and is scalable when the number of groups increases. The prototype results show that Grace achieves high accuracy when there is significant difference between intra-group and inter-group distances or when there is human shield as the blocking obstacle between groups.

The application scenario this work is targeting is that group members are face-to-face and are well separated from other groups by either distance or human shield. While one may view this as a major limitation, we argue that these proximity-based intentional groups have been neglected by existing work, yet identification of them is beneficial to many applications.

Acknowledgement

This project is supported in part by NSF grant CNS-0915574. We thank Alec Geatches for contributing to the initial stage of the prototype implementation.

References

[1] M. B. Kjargaard, M. Wirz, D. Roggen, and G. Troster, "Mobile sensing of pedestrian flocks in indoor environments using wifi signals," in *PerCom*, 2012.

[2] ——, "Detecting pedestrian flocks by fusion of multi-modal sensors in mobile phones," in *UbiComp*, 2012.

[3] D. Gordon, M. Beigl, M. Wirz, G. Troster, and D. Roggen, "Peer-to-peer group affiliation detection using mobile phones," Karlsruhe Institute of Technology, Tech. Rep., 2013, digbib.ubka.uni-karlsruhe.de/volltexte/documents/2800106.

[4] GPS.gov, "Gps accuracy," http://www.gps.gov/systems/gps/performance/accuracy.

[5] J. Xiao, K. Wu, Y. Yi, and L. M. Ni, "Fifs: Fine-grained indoor fingerprinting system," in *ICCCN*, 2012.

[6] C. Peng, G. Shen, Y. Zhang, Y. Li, and K. Tan, "Beepbeep: A high accuracy acoustic ranging system using cots mobile devices," in *SenSys*, 2007.

[7] H. Liu, Y. Gan, J. Yang, S. Sidhom, Y. Wang, Y. Chen, and F. Ye, "Push the limit of wifi based localization for smartphones," in *MobiCom*, 2012.

[8] S. Zhou and J. K. Pollard, "Position measurement using bluetooth," *IEEE Transactions on Consumer Electronics*, 2006.

[9] Z. Zhang, X. Zhou, W. Zhang, Y. Zhang, G. Wang, B. Y. Zhao, and H. Zheng, "I am the antenna: Accurate outdoor ap location using smartphones," in *MobiCom*, 2011.

[10] S. Sen, R. R. Choudhury, and S. Nelakuditi, "Spinloc: Spin once to know your location," in *HotMoile*, 2012.

[11] X. Li, J. Teng, Q. Zhai, J. Zhu, D. Xuan, Y. F. Zheng, and W. Zhao, "Ev-human: Human localization via visual estimation of body electronic interference," in *InfoCom*, 2013.

[12] N. Fet, M. Handte, and P. J. Marrn, "A model for wlan signal attenuation of the human body," in *Ubicomp*, 2013.

[13] L. Pei, R. Chen, J. Liu, H. Kuusniemi, T. Tenhunen, and Y. Chen, "Using inquiry-based bluetooth rssi probability distributions for indoor positioning," *Journal of Global Positioning Systems*, no. 2, 2010.

[14] C. Sagias and K. Karagiannidis, "Gaussian class multivariate weibull distributions: Theory and applications in fading channel," *IEEE Transactions on Information Theory*, pp. 3608–3619, 2005.

[15] A. Papoulis, *Probability, Random Variables, and Stochastic Processes*. McGraw-Hill Education, 2002.

[16] K. Yonekawa, J. Terayama, N. Namatame, J. Nakazawa, K. Takashio, and H. Tokuda, "Extracting a level of social relationship utilizing bluetooth signal with smartphones," in *UbiComp*, 2011.

[17] C. Bron and J. Kerbosch, "Algorithm 457: Finding all cliques of an undirected graph," *Communications of the ACM*, 1973.

[18] Wikipedia, "Jaccard index," http://en.wikipedia.org/wiki/Jaccard_index.

[19] J. Liu, Z. Wang, L. Zhong, J. Wickramasuriya, and V. Vasudevan, "uwave: Accelerometer-based personalized gesture recognition and its applications," in *PerCom*, 2009.

[20] BumpTechnologiesInc., "The bump app," http://bu.mp/company/.

[21] B. Guo, H. He, Z. Yu, D. Zhang, and X. Zhou, "Groupme: Supporting group formation with mobile sensing and social graph mining," in *Mobiquitous*, 2012.

[22] D. Roggen, D. Helbing, G. Troster, and M. Wirz, "Recognition of crowd behavior from mobile sensors with pattern analysis and graph clustering methods," *Networks and Heterogeneous Media*, pp. 521–544, 2011.

[23] D. Gordon, M. Scholz, Y. Ding, and M. Beigl, "Global peer-to-peer classification in mobile ad-hoc networks: A requirements analysis," in *CONTEXT*, 2011.

[24] D. Gordon, M. Scholz, and M. Beigl, "Group activity recognition using belief propagation for p2p mobile devices," Karlsruhe Institute of Technology, Tech. Rep., 2013, http://digbib.ubka.uni-karlsruhe.de/volltexte/1000036356.

[25] N. Banerjee, S. Agarwal, P. Bahl, R. Chandra, A. Wolman, and M. Corner, "Virtual compass: Relative positioning to sense mobile social interactions," in *Pervasive*, 2010.

[26] D. Kamisaka, T. Watanabe, S. Muramatsu, A. Kobayashi, and H. Yokoyama, "Estimating position relation between two pedestrians using mobile phones," in *Pervasive*, 2012.

[27] T. Higuchi, H. Yamaguchi, and T. Higashino, "Context-supported local crowd mapping via collaborative sensing with mobile phones," *Pervasive and Mobile Computing*, October 2013.

[28] S. Liu, Y. Jiang, and A. Striegel, "Face-to-face proximity estimation using bluetooth on smartphones," *IEEE Transactions on Mobile Computing*, March 2013.